

Interrogating the Cellular Impact of Sonodynamic Therapy on Glioma Cells

Justin N. Vinh^{a*}, Ryan T. Erny^{a*}, Andrew T. Thede^a, Matthew R. DeWitt^a, Natasha D. Sheybani^a

Group 9

^a Dept. of Biomedical Engineering, University of Virginia

*Authors contributed equally on this work

¹ Correspondence: nds3sa@virginia.edu | (434) 982-4269


Number of words:	3672
Number of figures and tables:	7
Number of equations:	1
Number of supplements:	3
Number of references:	21

ADVISOR

Dr. Natasha Sheybani, PhD

Assistant Professor, Dept. of Biomedical Engineering

Signature



Date

May 6, 2025

STUDENTS

Justin Vinh

Fourth-year Student, Dept. of Biomedical Engineering

Signature



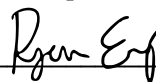
Date

May 6, 2025

Ryan Erny

Fourth-year Student, Dept. of Biomedical Engineering

Signature



Date

May 6, 2025

Interrogating the Cellular Impact of Sonodynamic Therapy on Glioma Cells

Justin N. Vinh^{1*}, Ryan T. Erny^{1*}, Andrew T. Thede¹, Matthew R. DeWitt¹, Natasha D. Sheybani^{1a}

¹ Dept. of Biomedical Engineering, University of Virginia

*Authors contributed equally on this work

^a Correspondence: nds3sa@virginia.edu | (434) 982-4269

Abstract

Glioblastoma (GBM) is one of the most common and deadly forms of adult brain cancers. Despite modern advances in surgical resection, chemotherapy, and radiotherapy, GBM outcomes have not substantially improved. Sonodynamic therapy (SDT) is a promising novel strategy taking advantage of tumor-specific accumulation of the sonosensitizing drug 5-ALA. SDT uses this accumulation in conjunction with exposure to focused ultrasound (FUS) to produce a selective therapy capable of killing malignant glioma cells. FUS is noninvasive and non-ionizing, making SDT especially advantageous compared to traditional treatment methods. While the use of SDT in GBM treatment is currently in clinical trials (including at the University of Virginia), to date, no study has systemically explored the cellular response of GBM to SDT. This gap in the literature hampers the developmental progress of SDT, so this in vitro study aimed to design an improved sonication staging system, systematically optimize treatment parameters, and characterize components released by GBM upon treatment. The improved staging mechanism was manually operated but allowed for simplified sonication operations while maintaining consistently reproducible FUS transducer placement. Thus far, this study has also generated several additions to a deeper understanding of 5-ALA-mediated SDT. A negative relationship between cell viability and higher FUS duty cycles and power settings was observed. However, results indicated that the sonication parameters 100 mV (450 kPa PNP) / 30% duty cycle / 5-min. duration were ideal for in vitro treatment, yielding 39% viability reduction relative to controls. Furthermore, the study observed that 1 mM of 5-ALA administered 4 hrs. prior to sonication yielded the best results considering experimental constraints. Finally, preliminary studies of GBM-derived extracellular vesicles (EVs) indicate a trend for sonication (both FUS and SDT groups) to yield higher concentrations of EVs with little to no effect on EV size.

Keywords: Glioblastoma (GBM), sonodynamic therapy (SDT), therapeutic focused ultrasound (FUS), 5-aminolevulinic acid (5-ALA), protoporphyrin IX (PpIX), extracellular vesicles (EVs)

Introduction

Glioblastoma (GBM) is one of the most prevalent and deadly types of brain cancer. Current leading standards of care include surgical resection, chemotherapy, and radiotherapy, but they do not significantly improve patient

outcomes, as only 5.8% of patients live 5 years post-diagnosis, with a median prognosis of only 12-15 months [1], [2]. The heterogeneity within the GBM cell population aids its ability to continually evade treatment and recur within patients. Recurrences of GBM often form less than 2 cm from previous resection areas, highlighting the fact that

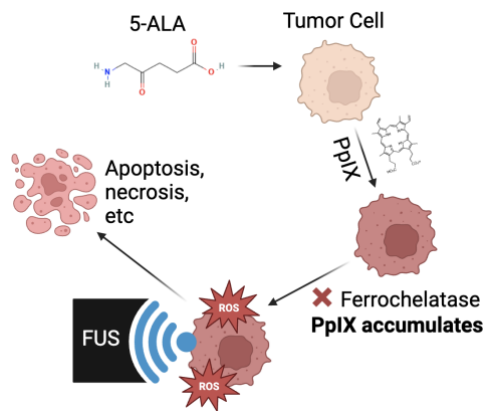


Figure 1. Mechanism of sonodynamic therapy used on tumor cells

highly robust surgical methods are often hindered by the highly variable profile of glioma stem cells (GSCs), a small but important subpopulation of GBM tumors [3].

Sonodynamic therapy (SDT) is a novel treatment combining the use of a sonosensitive drug and the application of therapeutic focused ultrasound (FUS). This therapy holds promise as a non-invasive and non-ionizing protocol that selectively targets glioma cells, potentially minimizing off-target effects present under current standards of care [4], [5]. The mechanisms of cell death imparted upon glioma cells by SDT are largely reported to be due to downstream processes resulting from the presence of sonosensitive drugs. Various drugs have been investigated, including 5-aminolevulinic acid (5-ALA) in facilitating SDT regimens [5]. 5-ALA in particular serves as an intermediate metabolite in the heme pathway, and accumulates as protoporphyrin IX (PpIX) in glioma cells due to decreased ferrochelatase expression among glioma cells (Fig. 1) [6]. Historically, 5-ALA has been used as a means to significantly improve gross tumor resection rates among clinical surgical procedures [3]. Oral administration of this drug prior to surgery induces fluorescent accumulation among the glioma cell population, aiding in the surgeon's ability to identify and resect malignant regions with greater specificity and resolution [3].

When used in SDT protocols, 5-ALA accumulates as PpIX, which is sensitive to sonication. Current leading hypotheses implicate the resulting cavitation effect and/or the production of reactive oxygen species (ROS), including singlet oxygen as primary drivers of cell death [4], [7]. Furthermore, existing research has shown that SDT induces glioma cell progression towards apoptotic pathways, as evidenced by enhanced Caspase 3 and Parp-1 expression [8]. It is also hypothesized that extracellular vesicles (EVs)

are secreted by glioma cells, modulating and suppressing immune responses [9]. However, existing studies have identified the ability of FUS regimens to modulate the profile of secreted EVs into an immunomodulatory one consistent with downregulation of classic cancer progression markers [10]. Notably, the literature lacks investigations involving the profiles of released EVs during SDT specifically. Furthermore, the reporting of ultrasound and cellular experimental parameters like duty cycle (DC), peak negative pressure (PNP), sonication duration, and sonosensitizer incubation time, and sonosensitizer dose are not consistently present in publications. This gap in the literature limits the ability of other researchers to robustly analyze and replicate successful existing SDT regimens and needs to be addressed.

Thus, this study will aim to 1) design a sonication platform that will better facilitate SDT in vitro studies, 2) characterize the cell viability response of GBM given different SDT parameters sets, and 3) analyze the secretome of SDT-treated GBM through the lens of EVs.

Results

Construction of a custom in vitro sonication platform

The successful execution of in vitro SDT experiments relies on the precise and replicable application of FUS across all experimental wells. The existing system was limited in its ability to perfectly control central transducer placement beneath each well and consisted of a motor translating the transducer along the XY planes. To both facilitate experiments and improve upon existing limitations, a novel sonication platform was designed and constructed.

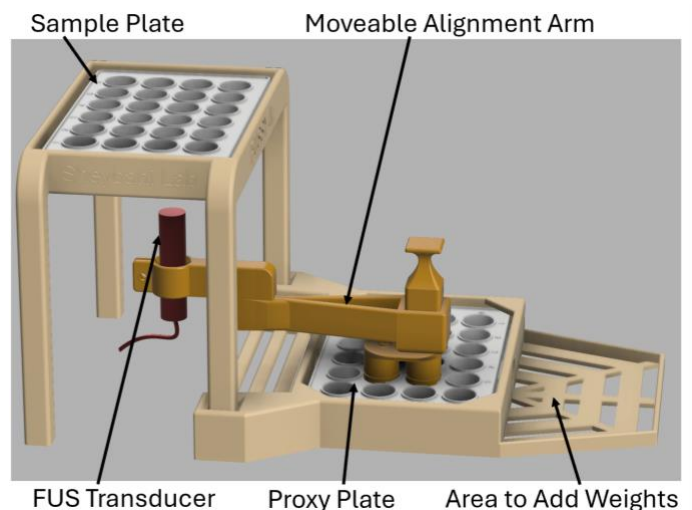


Figure 2. CAD render of custom in vitro sonication platform.

This system, dubbed FUSSY Jr., was designed using Fusion 360 and 3D printed with the goal of reducing the impact of human error while improving system performance and ease of use. Components of this design include the sample plate, proxy plate, alignment arm, FUS transducer, and weight holder areas (Fig. 2). This system enables its user to easily and manually transfer the transducer between wells with speed and precision. Manual movement of the alignment arm between sonications simply requires the user to pull the arm from the proxy plate and place it in the subsequent desired well. This process can be performed in seconds, and the alignment arm is designed to fit snugly into the wells to eliminate any movement. Line indentations are built into the alignment arm to confirm that the arm is fully secured within the well at the proper depth. The dual-plate layout, in conjunction with the alignment arm, ensures that the distance from the transducer remains constant. For the purposes of experiments, this distance was set at 22 mm. Measurements throughout experiments confirmed that this separation distance remained constant throughout the duration of the sonication time.

The proxy plate system also adequately controls the ideal central placement of the transducer. The length of the alignment arm was designed to place the transducer directly beneath the center of each well. Through this combination of transducer location control, the system enhances experimental replicability, reliability, and ease of use. Wells on the proxy plate correspond to those on the sample plate. Thus, moving the alignment arm to well A4, for instance, would place the transducer precisely under well A4 of the sample plate. Furthermore, this design was built with modularity in mind. 24-well plates were used in past experiments, but this system could easily support other plate sizes. The alignment arm also consists of two pieces, enabling the user to change the sonication field by changing the transducer distance from the well and/or conduct rapid calibration of the physical mount.

This system underwent an iterative process with an all-up testing approach. After initial testing, FUSSY Jr. v1 was determined to be too unwieldy to handle effectively and lacked the structural integrity needed to reliably maintain the transducer 22 mm from the well bottom. Instead, drooping on one end of the platform caused some wells to incur 18 mm of separation rather than 22 mm. These flaws were addressed, and FUSSY Jr. v2 was printed in a fraction of the time the first version required. Fig. 2 and S1 display a render and final print of this second version, which was smaller, sturdier, and included user-friendly features such as handholds and marking lines.

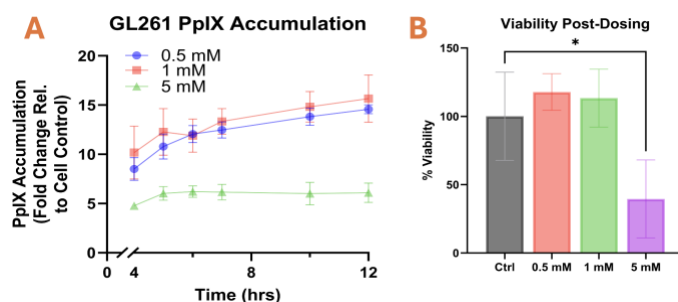


Figure 3. (A) The accumulation of 5-ALA as PpIX in GL251 cells over time with different doses. (B) Viability of GL261s cells at different doses 24 hrs. post-dosing. Results normalized to control viability.

PpIX accumulation is time- and dose-dependent

The uptake of 5-ALA was measured as the level of PpIX accumulation. GL261 cells were dosed with 5-ALA at 0.5 mM, 1 mM, and 5 mM doses, and PpIX accumulation was measured using a fluorescence plate reader at regular intervals over the span of 24 hrs. At 4 hrs. post-incubation, the 0.5, 1, and 5 mM doses had, relative to untreated controls, an average PpIX accumulation fold change of 8.51 ± 1.16 , 10.18 ± 2.68 , and 4.78 ± 0.28 , respectively (Fig. 3A). All dosing groups continued to accumulate PpIX until the 12 hrs. time point. At this point, the 0.5, 1, and 5 mM groups had PpIX accumulation fold changes of 14.58 ± 0.47 , 15.67 ± 2.40 , and 6.09 ± 1.00 , respectively. Furthermore, at nearly every time point, the 1 mM dose showed greater PpIX accumulation.

The average fold change for the 5 mM dose was substantially lower than the other two doses, so a viability assay was conducted at the 24 hr. time point to assess whether the 5 mM dose was inducing cytotoxic effects (Fig. 3B). Compared to the control, the 5 mM dose group experienced $60.5\% \pm 28.5\%$ reduction in viability compared to the untreated control ($p = 0.024$ using a one-way ANOVA with Tukey's multiple comparisons test.). The other two dosing groups did not experience differential viability relative to control. While the 12 hr. time point did show greater PpIX accumulation compared to the 4 hr. time point, the decision was made to use the 4 hr. time point in all SDT experiments due to practical experimental time considerations as well as clinical considerations.

SDT cytotoxicity is acoustic-parameter dependent

The attention of the study now turned to optimizing FUS acoustic parameters to maximize SDT cytotoxicity. These investigations focused on varying duty cycle, transducer power, and sonication duration. The duty cycle specifies how much time within a given period the transducer is actively producing ultrasound waves and is often denoted as

a percentage. The transducer power was set by the transducer signal generator and was specified in our studies in millivolts (mV). However, due to a multiple of variables impacting the transmission of ultrasound waves, a better measure for “power” of acoustic deposition is peak negative pressure (PNP), measured via a needle hydrophone. Measurements found that at the power settings chosen for experiments (80, 100, 120 mV), PNP varied linearly with power setting ($R^2 = 0.995$) (Fig. S2). This relationship can be described empirically using the following line of best fit:

$$\text{PNP(MPa)} = 0.0042 \times \text{Power(mV)} + 0.0346$$

As a starting point, the following parameters were chosen: 100 mV (450 kPa PNP), 30% duty cycle, and a 5 min sonication duration under SDT conditions. With these settings, significantly lower viability was observed in the SDT group relative to control. The average percent decrease in cell viability with respect to control in SDT, FUS-only, and 5-ALA-only groups was $38.9\% \pm 15.1\%$, $-5.5\% \pm 8.0\%$, and $5.2\% \pm 4.0\%$, respectively (Fig. 4). Of note, due to cell growth variability, viability for certain control groups relative to control can have $>100\%$ viability once normalized. However, groups expressing such features did not vary significantly from control and are, therefore, considered to be at 100% viability. The control groups of FUS and 5-ALA were both insignificantly different from each other, while each individually having significantly greater cell viability compared to SDT ($p < 0.0001$).

Through several parameter optimization experiments, a so-called “goldilocks zone” was discovered in which cell death was elicited when under SDT conditions, but not so among the other control conditions. Results from these early parameter tuning experiments are detailed in Fig. 5. Varying sonication duration was not seen to exhibit substantial

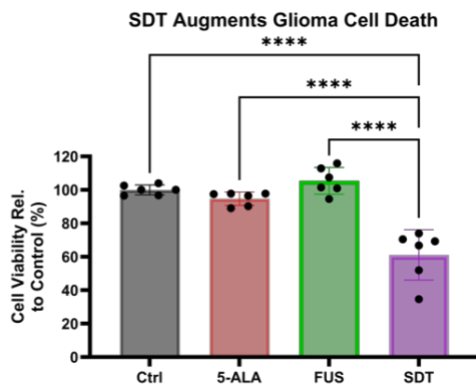


Figure 4. SDT elicits cell death, whereas each individual components of SDT (FUS and 5-ALA) do not within experimental parameters. 100 mV, 30% DC

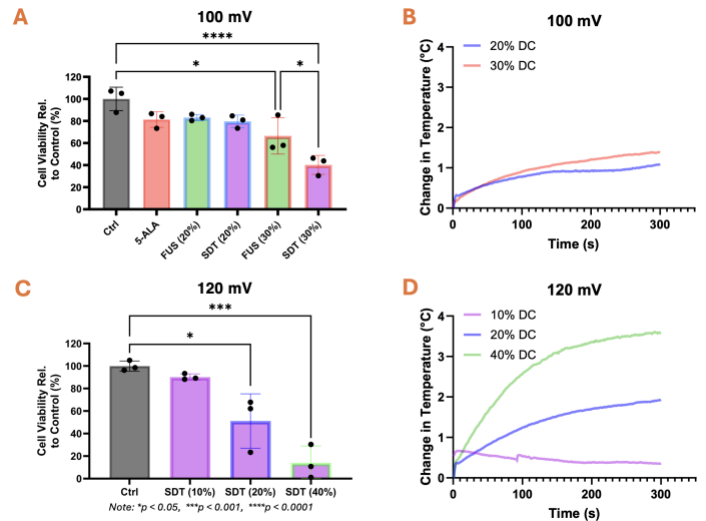


Figure 5. Parameter tuning experiments modulating power (mV) and duty cycle from (A) 100 mV and 20-30% DC and (B) 120 mV and 10-40% DC. (B, D) Representative thermocouple measurements show marginal increases in temperature from 37°C over the course of the sonication.

effects and are not detailed here. Of note, a pronounced increase in cell death under SDT conditions when duty cycle is increased was observed (Fig 5a, 5c). Likewise, for a given duty cycle, greater viability decrease was seen when used with a greater power regimen. Additionally, thermocouple measurements were taken to track changes in temperature experienced in the treated wells over the course of the sonication regimen. Lower duty cycle and power settings led to more minimal increases in temperature, but notably no sonication regimen increased the temperature by more than 4 °C. These experiments were all conducted at a standard starting temperature of 37°C, providing evidence that, indeed, non-thermal FUS was employed and that augmented cellular death is resultant from SDT and not a hyperthermic regime.

Extracellular vesicles show signs of modulation by SDT

EVs serve as molecular cargo carriers impactful in cellular signaling, but their role in modulating the tumor microenvironment of GBM prior to, during, and immediately after SDT treatment is largely unknown. In these preliminary experiments, EVs were isolated and showed a trend of increased concentrations of EV release when under sonication. Concentration in particles/mL ranged from $3.35 \times 10^7 \pm 7.50 \times 10^6$, $4.50 \times 10^7 \pm 9.97 \times 10^6$, $1.40 \times 10^7 \pm 2.37 \times 10^6$, and $1.80 \times 10^7 \pm 3.78 \times 10^6$ for SDT, FUS, 5-ALA, and control conditions, respectively (Fig. 6a). Note that Fig. 6 shows results from an $n = 1$ study, with error bars representing standard deviation of technical replicates (not biological replicates). The concentrations read were

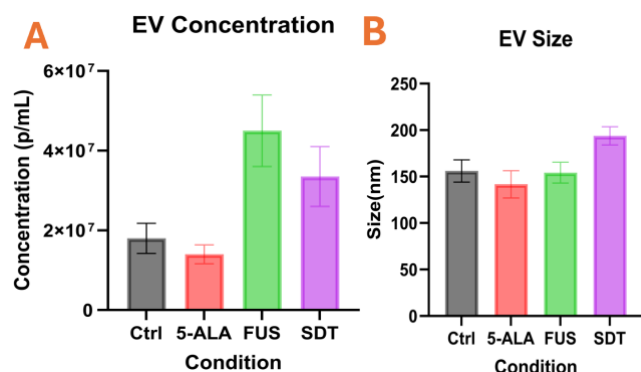


Figure 6. (A) EV concentration and (B) size. N=1, technical replicates were used to display error bars (SD).

near the lower limit of detection of the ZetaView nanoparticle tracking analysis system, which was on the order of 10⁷ particles/mL. Notably, these numbers were the result of already-pooled biological samples. Mean diameter (in nm) of the EVs was found as 193.88 ± 9.77, 154.24 ± 11.29, 141.70 ± 14.68, and 156.08 ± 12.01, respectively (Fig. 6b). Typical exosome size ranges from 30-100 nm in size [6], indicating that our isolation method may have allowed larger particles to pass through, skewing our results. The EVs were isolated using the ExoQuick-TC Ultra kit, and it is generally reported in the literature that differential ultracentrifugation (UC) is accepted as the “gold standard” for EV isolation [6].

Early trials with cancer stem cell-like glioma cells

Trials conducted with the GL261 cell line served as a preliminary experimental stage to identify and confirm successful execution of SDT within a “goldilocks” range of parameters. However, this adherent cell line is less indicative of the true in vivo GBM cell population. The G28 cell line represents a more stem cell-like model of GBM,

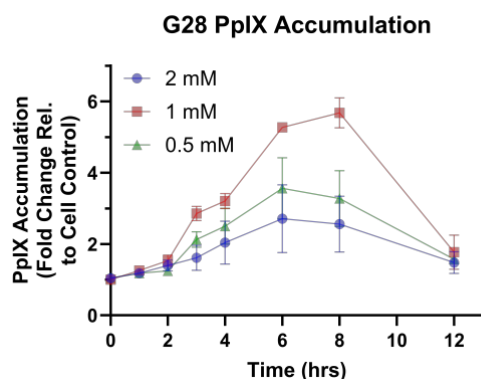


Figure 7. The accumulation of 5-ALA as PpIX in G28 cells over time with different doses.

forming 3D neurospheres in suspension, ultimately serving as a more clinically relevant model. Similar PpIX accumulation studies were performed with the cell line, revealing a 3-fold increase after 4 hours (Fig. 7). The lower accumulation compared to that of GL261 cells over the same time period highlights the evasive nature of in vivo GBM [11]. This is likely due to overexpression of ABCG2 transporters in GSCs, which facilitates the efflux of PpIX from the cells [12].

Discussion

Custom in vitro sonication platform controls variability

The construction of the custom in vitro sonication platform ultimately resulted in superior system ease of use, reducing both the experimental setup and run time, while increasing user confidence in consistent transducer placement via its proxy plate system and alignment arm markings. These important improvements allowed the user better control of the sonication field in between wells, maximizing the replicability of the system. Repeated measurements before, during, and immediately following sonication experimental runs confirmed that transducer distance did not change throughout. Furthermore, this platform benefits from its simple layout, as it requires little to no training for use. Its modular design also allows for plates with different numbers of wells to be substituted as desired, providing versatility across different experimental modes. These improvements over the existing system dramatically facilitated the conduction of the subsequent successful parameter tuning experiments. Adequate transducer location control may be responsible for reductions in variability within groups, as this system maintained consistent sonication fields across wells.

Parameter tuning elucidates ideal in vitro SDT regimen

Several experimental parameters were investigated in order to address the lack of robust data in the literature [13]. These parameters included cell seeding density, 5-ALA dose concentration, incubation time, FUS power, duty cycle, and sonication time. Timing, seeding, and dosing studies were first conducted to identify optimal PpIX accumulation with the goal of ultimately accentuating the SDT effect (Fig. 3A). While a 1 mM dose and 4 hour incubation period were found to produce optimal accumulation, higher doses were investigated and even found to have a cytotoxic effect at 5 mM. This was supported by the significant decrease in cell viability 24 hours post-dosing at this concentration. After confirming the optimal efficacy of cellular-associated parameters, FUS power and duty cycle were explored. Initial studies provided evidence that high-power, high-

duty-cycle sonications significantly reduced cell viability (Fig. 5c). However, these observations were approached cautiously, as the FUS-only control group also yielded a significant decrease in cell viability compared to an untreated control. This provided evidence that cell death within the SDT experimental group may be confounded by an overly powerful sonication regimen. It is hypothesized that mechanical disturbances like cell shearing, introduced via these more aggressive regimens, may be responsible for this cell death rather than traditional SDT mechanisms. These concerns were supported by visual evidence of media being expelled from the well during sonication, and microscopic images of sheared cells post-sonication (Fig. S3). Reducing FUS power and duty cycle eliminated these observations and yielded significant decreases in cell viability compared to various control groups while preventing cell shearing from the well bottom (Fig. 5a). Thermocouple measurements were also obtained, providing evidence that increases in temperature resulting from sonication were marginal and unlikely to have played a role in eliciting cell death [14]. Cell viability in the SDT group was significantly less than that of all other groups. Additionally, all control monotherapies were insignificantly different compared to one another, providing evidence that the FUS regimen was not eliciting cell death on its own.

EV release may be augmented during SDT

The underlying mechanisms of SDT involve complex cell signaling processes that are in some capacity carried out by EVs [9], [15], [16]. In order to determine exactly what role EVs play in GBM progression, inhibition, or immunomodulation [10] during SDT, the ExoQuick-TC Ultra isolation kit was used as a means to extract them from treated cells in media. Fetal bovine serum (FBS) depleted media was used to eliminate contamination [17], and samples across wells were pooled before examination using the ZetaView nanoparticle tracking analysis instrument. EV concentration showed a trend of increased density within sonicated groups (Fig. 6a), however, the values were notably near the lower limit of detection for the instrument. These results were also limited by an $n = 1$ sample size. Furthermore, mean EV size was observed to be above what is traditionally known to be the upper limit of true exosome size (30-100 nm), suggesting that our method of isolation may not have been fully robust [6]. These EV data sets represent preliminary explorations into the secretome, whereas future experiments plan to further illustrate the molecular EV and cytokine profile, including various interleukins, TNF, PD-L1, as well as secretions from different cell types including GSCs [18], [19], [20], [21].

Recent studies have shifted towards differential ultracentrifugation as a means of EV isolation, widely regarded as the optimal method [6].

Materials and Methods

Cell culture

The murine glioma cell line GL261 was obtained from the Sheybani Lab at the University of Virginia (UVA). The GL261 line was cultured in DMEM with 4.5 g/L glucose, sodium pyruvate, L-glutamine, and 10% FBS. The human glioma stem cell-like line G28 was obtained from the Abounader Lab likewise at UVA. The G28 line was cultured as suspended 3D neurospheres in neurobasal medium with 0.5X L-glutamine, 0.5X B27, 0.5X N2, 50 ng/mL human bFGF, and 50 ng/mL human EGF. All cells were incubated at 37 °C and 5% CO₂.

Protoporphyrin IX accumulation

To measure protoporphyrin IX (PpIX) accumulation, cells were seeded in CoStar black 96-well plates and dosed with the appropriate amount of 5-ALA (Sigma Aldrich) dissolved in media. G28 cells were dosed 72 hrs. post-seeding, while GL261 cells were dosed 24 hrs. post-seeding. The uptake of 5-ALA was measured as the metabolic conversion and accumulation of PpIX, measured fluorescently using the Griffin Lab BioTek Synergy H1 reader (405 nm excitation, 636 nm emission, auto-gain “ON”). Measurements were made at regular intervals between 0.5 hrs. and 24 hrs. Samples were kept in the dark between measurements.

Sonodynamic therapy

Sonication was conducted using a 1 cm diameter unfocused transducer operated at 1.1 MHz. Relevant sonication parameters ranged 80-120 mV, 10%-40% duty cycle, and 5 minute duration. Samples were placed in clear 24-well plates wrapped in parafilm and partially submerged in 37 °C degassed water.

Cells were seeded either 5 hrs. or 24 hrs. prior to sonication. Dosing was completed by dissolving 5-ALA (Sigma Aldrich) in media before being administered at the proper dosage to samples 4 hrs. prior to sonication. All procedures were conducted in the dark.

Cell viability assay

Cell viability was determined using the CellTiter-Glo® Luminescent Cell Viability Assay (Promega). Measurements of the samples, along with the requisite standards, were made in CoStar white flat bottom 96-well

plates using the luminescence reader maintained by the Abeyayehu Lab. The assay was added 1:1 with samples and given 15 minutes to incubate at room temperature prior to readings. Measurements were set to use 1000 ms integration time.

Extracellular vesicles

Extracellular vesicles (EVs) were isolated using ExoQuick-TC Ultra kits. Samples marked for EV isolation had their media swapped for an FBS(-) version immediately prior to sonication. Samples were allowed to incubate for 30 minutes post-sonication before the supernatant was extracted for EV isolation. After isolation, the size and concentration of EVs within samples were measured using a ZetaView nanoparticle tracking analysis device.

FUSSY Jr. design and construction

The FUSSY Jr. sonication platform was modeled computationally using Autodesk Fusion 360, sliced using UltiMaker Cura software, and predominately printed on the UltiMaker S3.

Statistics and Software

All graphs and statistical analyses were conducted using GraphPad Prism and Microsoft Excel. Pairwise comparisons used a one-way ANOVA followed by Tukey's multiple comparison test. Unless otherwise indicated, graphical error bars as well as in-text error ranges represent ± 1 standard deviation (SD) from the mean (M). Significance is defined as exhibiting a p-value below $\alpha = 0.05$.

End Matter

Author Contributions and Notes

J.N.V and R.T.E designed research, performed research, analyzed data, created all graphs, and wrote the paper.

A.T.T characterized EVs and provided guidance in downstream EV analysis. M.R.D assisted in the conducting of sonications for SDT and in the design of FUSSY Jr.

The authors declare no conflict of interest.

Acknowledgments

J.N.V and R.T.E would like to acknowledge the mentorship and guidance that N.D.S has provided throughout the entirety of the capstone process. Through her guidance, the paper's authors have grown considerably as scientists, more confident in their abilities and critical thinking skills.

J.N.V and R.T.E would also like to acknowledge the funding sources that made this research possible, including

(but not limited to) the UVA Comprehensive Cancer Center Neuro-Translational Research Team Pilot Award, the Raven Society Fellowship, and the Harrison Undergraduate Research Award.

References

- [1] W. Diao *et al.*, "Behaviors of Glioblastoma Cells in in Vitro Microenvironments," *Sci. Rep.*, vol. 9, no. 1, p. 85, Jan. 2019, doi: 10.1038/s41598-018-36347-7.
- [2] A. C. Tan, D. M. Ashley, G. Y. López, M. Malinzak, H. S. Friedman, and M. Khasraw, "Management of glioblastoma: State of the art and future directions," *CA. Cancer J. Clin.*, vol. 70, no. 4, pp. 299–312, Jul. 2020, doi: 10.3322/caac.21613.
- [3] S. Eljamel, "5-ALA Fluorescence Image Guided Resection of Glioblastoma Multiforme: A Meta-Analysis of the Literature," *Int. J. Mol. Sci.*, vol. 16, no. 5, Art. no. 5, May 2015, doi: 10.3390/ijms160510443.
- [4] K. Bilmin, T. Kujawska, and P. Grieb, "Sonodynamic Therapy for Gliomas. Perspectives and Prospects of Selective Sonosensitization of Glioma Cells," *Cells*, vol. 8, no. 11, Art. no. 11, Nov. 2019, doi: 10.3390/cells8111428.
- [5] K. M. Nowak, M. R. Schwartz, V. R. Breza, and R. J. Price, "Sonodynamic therapy: Rapid progress and new opportunities for non-invasive tumor cell killing with sound," *Cancer Lett.*, vol. 532, p. 215592, Apr. 2022, doi: 10.1016/j.canlet.2022.215592.
- [6] F. Momen-Heravi, "Isolation of Extracellular Vesicles by Ultracentrifugation," in *Extracellular Vesicles: Methods and Protocols*, W. P. Kuo and S. Jia, Eds., New York, NY: Springer, 2017, pp. 25–32. doi: 10.1007/978-1-4939-7253-1_3.
- [7] T. Kitagawa *et al.*, "5-Aminolevulinic acid strongly enhances delayed intracellular production of reactive oxygen species (ROS) generated by ionizing irradiation: Quantitative analyses and visualization of intracellular ROS production in glioma cells in vitro," *Oncol. Rep.*, vol. 33, no. 2, pp. 583–590, Feb. 2015, doi: 10.3892/or.2014.3618.
- [8] K. Sheehan *et al.*, "Investigation of the tumoricidal effects of sonodynamic therapy in malignant glioblastoma brain tumors," *J. Neurooncol.*, vol. 148, no. 1, pp. 9–16, May 2020, doi: 10.1007/s11060-020-03504-w.
- [9] V. Indira Chandran, S. Gopala, E. H. Venkat, M. Kjolby, and P. Nejsum, "Extracellular vesicles in glioblastoma: a challenge and an opportunity," *Npj Precis. Oncol.*, vol. 8, no. 1, pp. 1–8, May 2024, doi: 10.1038/s41698-024-00600-2.
- [10] N. D. Sheybani, A. J. Batts, A. S. Mathew, E. A. Thim, and R. J. Price, "Focused Ultrasound Hyperthermia Augments Release of Glioma-derived Extracellular Vesicles with Differential Immunomodulatory Capacity," *Theranostics*, vol. 10, no. 16, pp. 7436–7447, Jun. 2020, doi: 10.7150/thno.46534.
- [11] Z.-Y. Xu, X.-Q. Li, S. Chen, Y. Cheng, J.-M. Deng, and Z.-G. Wang, "Glioma Stem-like Cells are Less Susceptible than Glioma Cells to Sonodynamic Therapy with Photofrin," *Technol. Cancer Res. Treat.*, vol. 11, no. 6, pp. 615–623, Dec. 2012, doi: 10.7785/tcrt.2012.500277.
- [12] Z.-Y. Xu *et al.*, "The ABCG2 transporter is a key molecular determinant of the efficacy of sonodynamic therapy with Photofrin in glioma stem-like cells," *Ultrasonics*, vol. 53, no. 1, pp. 232–238, Jan. 2013, doi: 10.1016/j.ultras.2012.06.005.
- [13] A. Keenlyside *et al.*, "Development and optimisation of in vitro sonodynamic therapy for glioblastoma," *Sci. Rep.*, vol. 13, no. 1, p. 20215, Nov. 2023, doi: 10.1038/s41598-023-47562-2.

- [14] D. Ju *et al.*, "Hyperthermotherapy enhances antitumor effect of 5-aminolevulinic acid-mediated sonodynamic therapy with activation of caspase-dependent apoptotic pathway in human glioma," *Tumor Biol.*, vol. 37, no. 8, pp. 10415–10426, Aug. 2016, doi: 10.1007/s13277-016-4931-3.
- [15] P. S. Jones *et al.*, "Characterization of plasma-derived protoporphyrin-IX-positive extracellular vesicles following 5-ALA use in patients with malignant glioma," *eBioMedicine*, vol. 48, pp. 23–35, Oct. 2019, doi: 10.1016/j.ebiom.2019.09.025.
- [16] A. Mondal, D. Kumari Singh, S. Panda, and A. Shiras, "Frontiers | Extracellular Vesicles As Modulators of Tumor Microenvironment and Disease Progression in Glioma", doi: 10.3389/fonc.2017.00144.
- [17] R. R. Khasawneh, A. H. Al Sharie, E. Abu-El Rub, A. O. Serhan, and H. N. Obeidat, "Addressing the impact of different fetal bovine serum percentages on mesenchymal stem cells biological performance," *Mol. Biol. Rep.*, vol. 46, no. 4, pp. 4437–4441, Aug. 2019, doi: 10.1007/s11033-019-04898-1.
- [18] P. Jarmuzek, P. Defort, M. Kot, E. Wawrzyniak-Gramacka, B. Morawin, and A. Zembron-Lacny, "Cytokine Profile in Development of Glioblastoma in Relation to Healthy Individuals," *Int. J. Mol. Sci.*, vol. 24, no. 22, p. 16206, Nov. 2023, doi: 10.3390/ijms242216206.
- [19] T. Lokumcu *et al.*, "Proteomic, Metabolomic, and Fatty Acid Profiling of Small Extracellular Vesicles from Glioblastoma Stem-Like Cells and Their Role in Tumor Heterogeneity," *ACS Nano*, vol. 18, no. 3, pp. 2500–2519, Jan. 2024, doi: 10.1021/acsnano.3c11427.
- [20] F. L. Ricklefs *et al.*, "Immune evasion mediated by PD-L1 on glioblastoma-derived extracellular vesicles," *Sci. Adv.*, vol. 4, no. 3, p. eaar2766, Mar. 2018, doi: 10.1126/sciadv.aar2766.
- [21] C. Spinelli *et al.*, "Molecular subtypes and differentiation programmes of glioma stem cells as determinants of extracellular vesicle profiles and endothelial cell-stimulating activities," *J. Extracell. Vesicles*, vol. 7, no. 1, p. 1490144, 2018, doi: 10.1080/20013078.2018.1490144.

Supplemental Materials

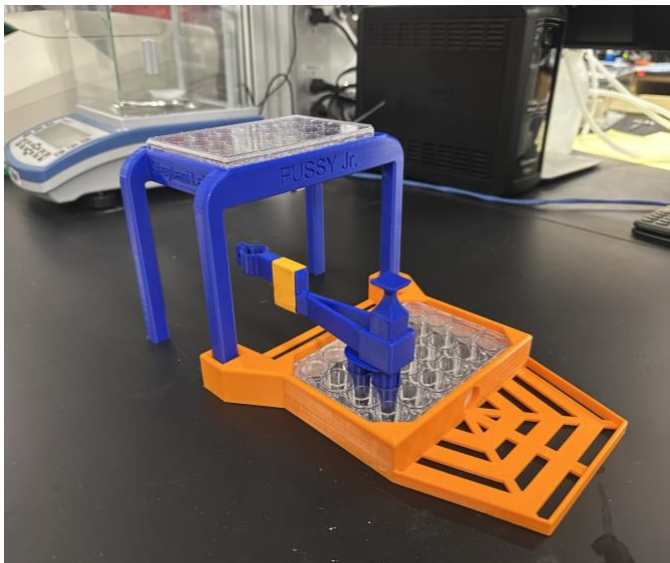


Figure S1. Final printed version of custom in vitro sonication platform, shown with sample and proxy plates present.

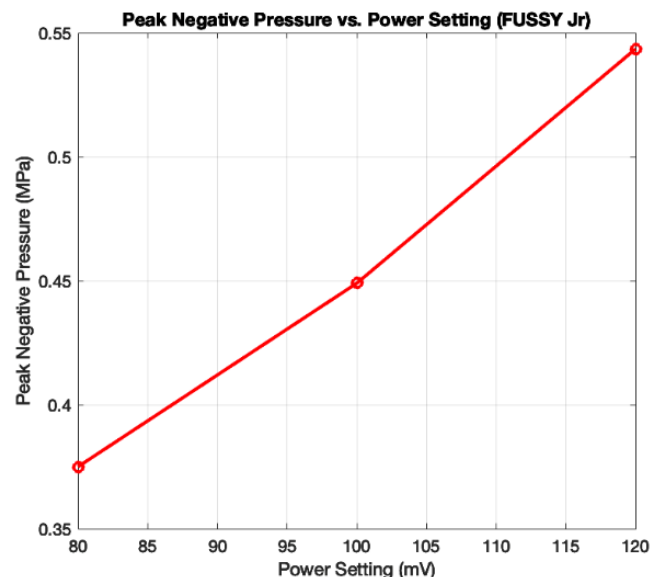


Figure S2. Relationship between peak negative pressure (PNP) in MPa and power setting (mV).



Figure S3. Microscopy images of untreated control (Left), FUS (Middle), and SDT (Right) groups 30 minutes post-treatment at aggressive regimen (120 mV, 40% DC, 5 min.).